

# Infrared thermography for prediction of spontaneous combustion of sulfide ores

LI Zi-jun, SHI Dong-ping, WU Chao, WANG Xiao-lei

School of Resources and Safety Engineering, Central South University, Changsha 410083, China

Received 9 September 2011; accepted 17 October 2011

**Abstract:** The method of infrared thermography to predict the temperature of the sulfide ores has a large error. To solve this problem, the temperature of the sulfide ores is measured by thermal infrared imager and recording thermometric instrument contrastively. The main factors, including emissivity, distance, angle and dust concentration that affect the temperature measurement precision, are analyzed. The regression equations about the individual factors and comprehensive factors are obtained by analyzing test data. The application of the regression equations improves the precision of the thermal infrared imager. The geometric information lost in traditional infrared thermometry is determined by visualization grid method and interpolation method, the relationship between the infrared imager and geometry information is established. The geometry location can be measured exactly.

**Key words:** sulfide ores; spontaneous combustion; prediction; infrared thermography; influent factors; regression equations; geometry location

## 1 Introduction

The spontaneous combustion of sulfide ores will bring huge economic loss and cause a series of environmental and safety problems. So it has positive significance to predict the spontaneous combustion of sulfide ores.

There are several methods which are applicable to the prediction of spontaneous combustion of sulfide ores, such as the thermal couple method and gas detection method. However, these traditional methods are complicated, high-cost and have large error. Infrared thermometry method has many convenient advantages. Its features for non-contact measurement effectively avoid the staff and harmful gas direct contact. The application of infrared thermometry in sulfide ores has been studied. This research promoted the development of infrared technology in sulfide ores [1–4].

On the basis of previous studies, the factors that affect the infrared thermometry were studied in detail, and the influence of dust was pulled in innovative. Regression equations that could revise the measured value were obtained. The physical location was determined by visual grid method and interpolation method.

## 2 Experimental

### 2.1 Sample preparation and analysis

There were four typical samples which were collected in mine in this experiment. The multi-drop sampling method was used in sulfide ores collection. Table 1 indicates the chemical composition of the four sulfide ores concentrates.

### 2.2 Test instruments

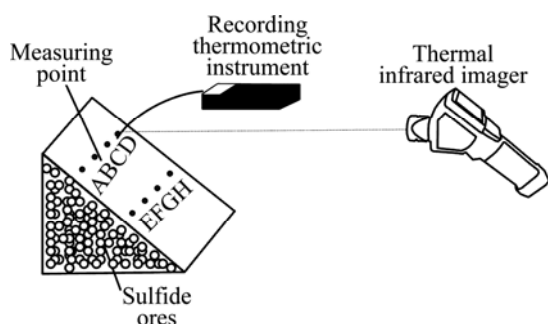
The test instruments included IRI1011 Infrared thermal imager, CENTER recording thermometric instrument, LD-3C microcomputer laser dust apparatus, HANBA Programmable high-temperature experiment box.

### 2.3 Test stockpile

Due to the need of experiment, the sulfide ores were crushed. The particle diameter was grinded to less than 40 mm. The physical model of laboratory was built for wedge in laboratory. The length of the ore heap was about 150 mm, the width was about 100 mm, the height was about 80 mm, and the angle was 35°. The experimental devices are shown in Fig. 1.

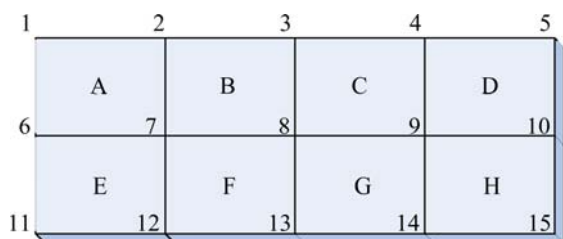
**Table 1** Chemical composition of sulfide concentrates

Sample No.	Chemical composition/%			
	S <sup>0</sup>	SO <sub>4</sub> <sup>2-</sup>	TS	Water-soluble Fe <sup>2+</sup> and Fe <sup>3+</sup>
A	0.044	1.57	35.27	0.0016
B	0.044	1.55	33.41	0.0008
C	0.320	2.66	48.02	0.2300
D	0.140	1.70	40.70	0.2000

**Fig. 1** Schematic diagram of experimental device

## 2.4 Test method

The square grids with the side length of 20 mm were made by grid lines in the lateral surface of the sulfide heap. There were total 4×2 square grids in the surface. Each node of the grids was set to an infrared measuring point, and there were 15 infrared measuring points, and the numbers were set to 1, 2, 3, ..., 15. Each center of the grids was set to the measuring point and there were 8 measuring points, and the numbers were set to A, B, C, ..., H. These 8 measuring points were infrared measuring points by recording thermometric instrument. The distribution of measuring points is shown in Fig. 2.

**Fig. 2** Distribution map of measuring points

The temperature recorded by memory-type thermometer was seen as the real temperature, and the temperature recorded by infrared thermometry was analyzed on error. The environment of mine was simulated in laboratory. Contrast temperature measurement was performed under conditions of different distances, angles and dust concentrations. The regression analysis was applied to the temperature measurement results, the regression equations were obtained, and the temperatures of the measuring points of 1 to 15 were amended by regression equations. The

visualization grid method was applied to the modified temperature, and the geometric information was obtained. It provides the basis for the acquisition of measuring points' geometric coordinates [5–7].

## 3 Influencing factors analysis and correction

The accuracy of temperature measurement of infrared thermometry has relationship with the emissivity of measured object, temperature measuring distance, temperature measuring angle, dust concentration of measurement temperature environment. More accurate value of the infrared temperature measurement can be gotten only if the factors influencing the measuring results are found.

### 3.1 Emissivity

The temperature measured by infrared thermometry is not the real temperature of object but the radiation temperature. The real temperature can be received according to the radiation temperature when we know the emissivity. The emissivity of sulfide ores is related to the surface condition, roughness, oxidation degree and so on.

The method of measuring the emissivity of sulfide ores was to record the temperature of measuring points by infrared thermometry and memory-type thermometer. The temperature obtained by memory-type thermometer was the real temperature of object. The temperature obtained by infrared thermometry was the radiation temperature. The emissivity of sulfide ores can be acquired according to the comparison of the real temperature and radiation temperature. Figure 3 shows the infrared thermography under the situations of taking into account the emissivity and not taking into account the emissivity. The emissivity of sample ore A is 0.89. Table 2 shows the emissivities of the four sample ores worked out by comparison and contrast.

Emissivity is the inherent properties of the measured object, so we cannot change it. However, when the infrared thermography is applied to the practical work, we can take the measured sulfide ores samples in advance. The emissivity of the infrared thermography can be modified on the basis of the emissivity measured. The purpose of improving the measurement accuracy is achieved [8,9]

### 3.2 Impact of distance

The distance between the infrared thermography and the measured object has a significant effect on measuring accuracy. The low accuracy, on one hand, is due to the fact that the atmospheric penetration rate decreases with distance; on the other hand, it is due to the fact that the object has not been fully filled with the

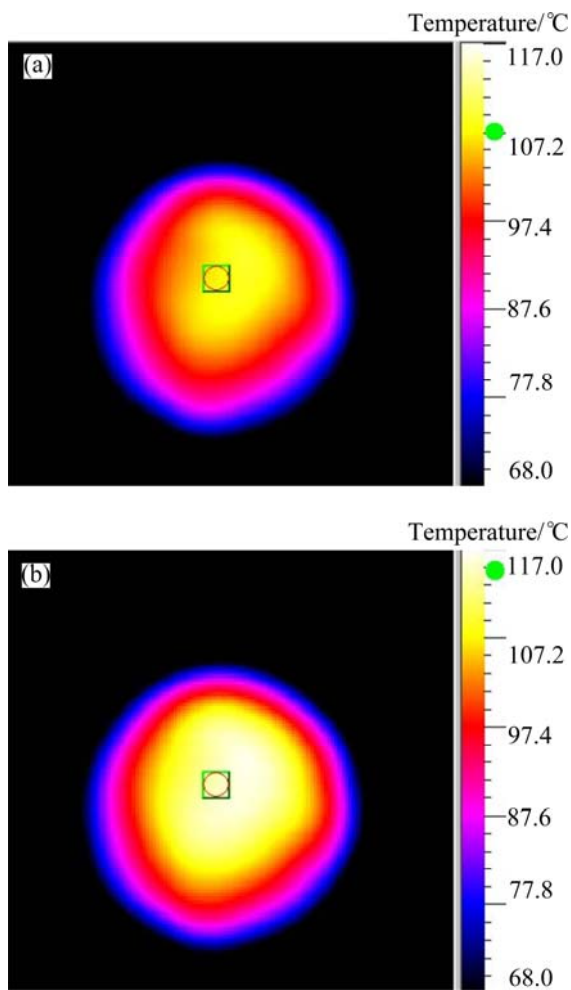


**Fig. 3** Infrared image of sample A: (a) Taking emissivity into account; (b) Not taking emissivity into account

**Table 2** Emissivity of four samples

Sample No.	A	B	C	D
Emissivity	0.89	0.91	0.85	0.93

view field, and the output signal is too low. We took the measured data of the A sample ore for examples. The influencing law of the distance on the temperature measured by infrared thermography was detected (Fig. 4).

We can see from Fig. 4 that with the increase of distance, the relative error of the temperature measured by infrared thermography gradually increases. The regression equations about the temperature affected by distance were attained. The regression equations of the four sample ores are shown in Table 3.

We can draw a conclusion from the analysis of the test data that the farther the distance is, the bigger the error between the temperature measured by infrared thermography and the real temperature. Therefore, we can modify the error by the application of the regression equations in Table 3 [10–12].

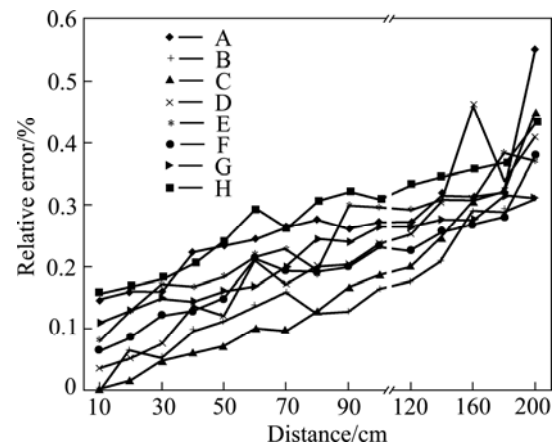


**Fig. 4** Relative error of sample A affected by distance

**Table 3** Regression equations of samples affected by distance

Sample No.	Regression equation	Equations No.
A	$y = -0.197a - 0.0192b + 73.713$	(1)
B	$y = 0.297a + 0.0182b + 55.554$	(2)
C	$y = 0.691a + 0.122b + 39.983$	(3)
D	$y = -0.057a - 0.008b + 77.229$	(4)

*a* is the temperature measured by thermal infrared imager; *b* is the distance.

### 3.3 Impact of angle

The measuring angle also has a great influence on the temperature measured by infrared thermography. The error becomes large with the increase of the angle. The angle between the thermal infrared imager lens and the surface normal direction of the sulfide ores is 90°. In the actual measurement, due to the characteristics of the ore body itself, the measuring angle may be very big, so the measuring error is large. The modification of the relative error is needed.

Taking point A in sample A for an example, the relative error of the measuring angle is shown in Fig. 5.

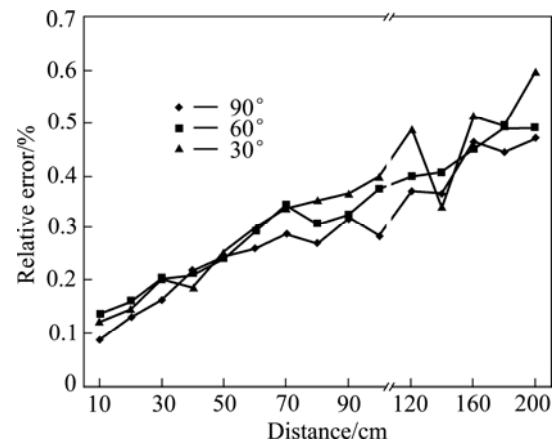


**Fig. 5** Relative error of sample A affected by angle

The experiment was made under the condition that the angles between the thermal infrared imager lens and the surface normal direction of the ores are 90°, 60° and 30°, respectively. With the increase of the angle between the thermal infrared imager lens and the surface normal direction of the ores, the relative error becomes large. In order to attain the regression equations of the four ore samples about the angle, the test data were analyzed. Table 4 shows the regression equations by just considering the angle effect.

**Table 4** Regression equations of samples affected by angle

Sample No.	Regression equation (not taking distance into account)	Equation No.
A	$y=-0.04a+0.002c+54.886$	(5)
B	$y=-0.025a+0.001c+66.985$	(6)
C	$y=0.081a-0.004c+57.685$	(7)
D	$y=0.048a-0.002c+78.291$	(8)

$a$  is the temperature measured by thermal infrared imager;  $c$  is the angle.

The experiment was made when the angles between the thermal infrared imager lens and the surface normal direction of the ores were 90°, 60° and 30°. We can see that, when the angle was 90°, the relative error was small. Therefore, when we use the infrared thermography in practical situation, we make sure the infrared imager lens vertical to the measuring point where the ores surface is normal to it. If we cannot guarantee that the angle can reach the angle of 90°, the angle must be controlled in the scale of 30°. Also, we can use the regression equations to modify the error generated by the angle [13,14].

### 3.4 Impact of dust concentration

The dust and suspended particles in the environment will also cause the attenuation of the infrared radiation in the process of their propagate in the air. These particles on the absorption of infrared radiation may lead to attenuation of radiation capacity. There is large dust in the mine operation environment, therefore studying the impact of the dust concentration on the infrared thermography has a positive significance.

Under the laboratory condition, the dust concentration was less than 0.9 mg/m<sup>3</sup>. Table 5 shows the regression equations of the four ores samples by only considering the effect of the dust concentration.

The more harsh the measuring environment is, the more the decrease of the infrared radiation is, then the relative error will become large. When using the thermal infrared imager under the mine, the right band of the infrared imager should be chosen. We can also modify the relative error by the regression equations. We should control the error to a minimum.

**Table 5** Regression equations of samples affected by dust concentration

Sample No.	Regression equations (not taking distance into account)	Equation No.
A	$y=0.185a-6.594d+74.765$	(9)
B	$y=0.397a+8.929d+39.985$	(10)
C	$y=0.001a-0.976d+73.771$	(11)
D	$y=0.396a+4.446d+56.925$	(12)

$a$  is the temperature measured by thermal infrared imager;  $d$  is the dust concentration

### 3.5 Comprehensives impact

The factors affecting the precision of the thermal infrared imager in the practical sulfide ores had been studied. The test data were analyzed comprehensively, and then the regression equations of the four sulfide ores samples were attained, considering the comprehensive effect of distance factor, angle factor, dust concentration factor. The regression equations are shown in Table 6.

**Table 6** Regression equations of samples affected by distance, angle and dust concentration

Sample No.	Regression equation	Equation No.
A	$y=0.154a+0.026b-0.021c-5.303d+73.779$	(13)
B	$y=-0.204a-0.045b+0.031c-2.641d+65.55$	(14)
C	$y=0.668a+0.128b-0.06c-3.931d+32.754$	(15)
D	$y=0.627a+0.109b-0.055c+5.437d+16.981$	(16)

$a$  is the temperature measured by thermal infrared imager;  $b$  is the distance;  $c$  is the angle;  $d$  is the dust concentration.

Taking the distance, angle and dust concentration into account, the elements affecting the measure of the thermal infrared imager could be considered in the regression equations of the sulfide ores. In the practical work, by taking the actual values of the distance, angle, dust concentration into the regression equation, the result can be worked out after modification. With the appliance of the comprehensive regression equation, the temperature errors of the thermal infrared imager greatly decrease.

### 3.6 Application

By applying the regression equations of the four sulfide ores to the actual work, the real application was proceeded in the sampling site. These measuring points a, b, c, d, respectively, are near the sampling site of sample A, B, C and D. The measuring points a, b, c, d were measured by thermal infrared imager, and the corrected value calculated by regression equations was compared with real value. The relative error can be seen.

The infrared images of measuring points a, b, c, d are shown in Fig. 6. These infrared images have taken emissivity into account.

Table 7 shows that after calculating of the regression equations, the relative error between the corrected temperature value and the real temperature measured by recording thermometric instrument become small. This improved the measurement accuracy of the

final result.

However, the regression equations obtained in the experiment have limitations. The regression equations only apply to the situation that the emissivity of the measured ores is the same as that of A, B, C or D sulfide ores. If the emissivity of the measured sulfide ores is unknown, the experiment must be done again to draw a new regression equation.

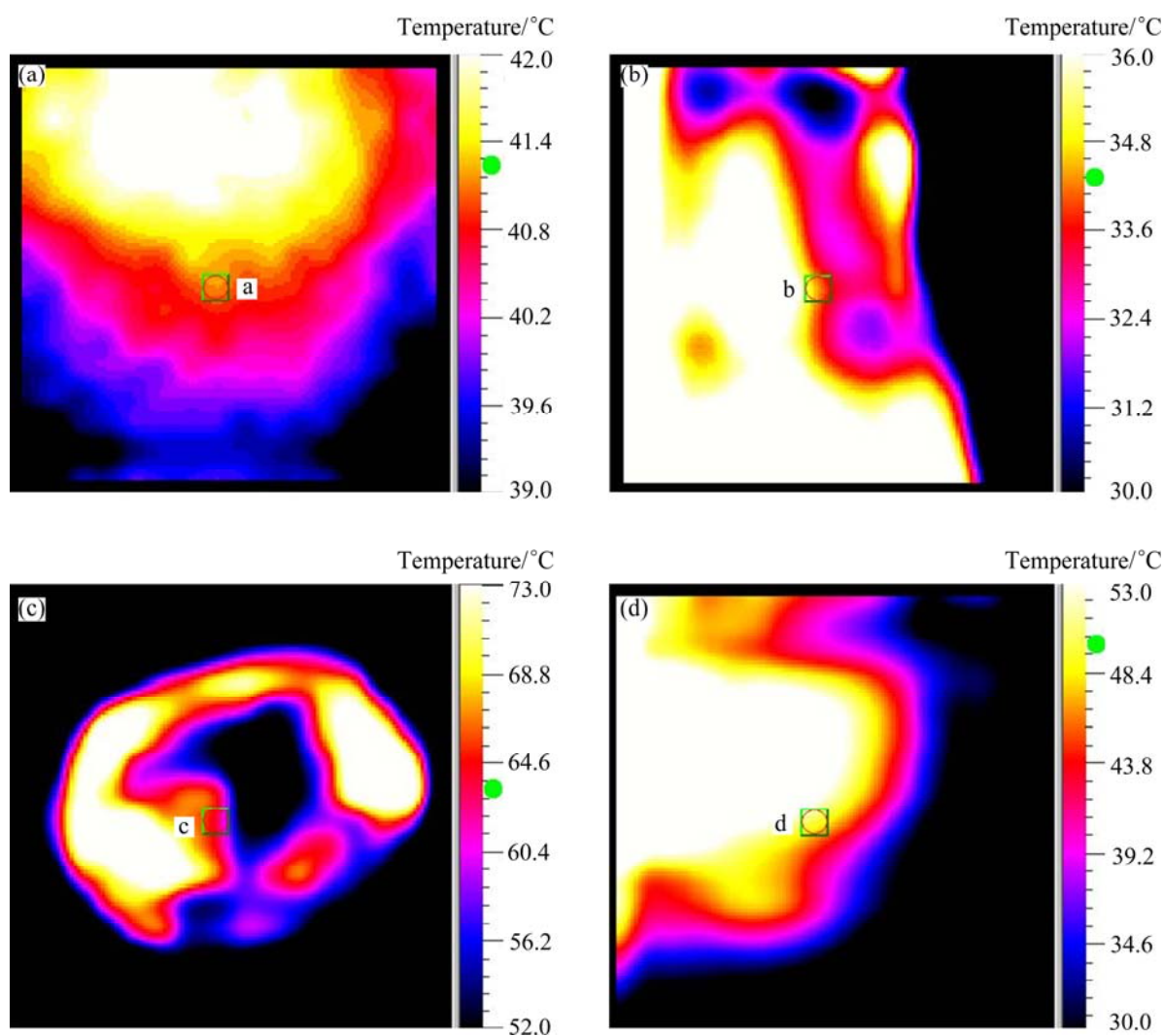


Fig. 6 Infrared images of measuring points a (a), b (b), c (c) and d (d)

Table 7 Comparison of real value and corrected value

Measuring point	Temperature/°C			Relative error/%		Measuring distance/cm	Measuring angle/(°)	Measuring dust concentration/(mg·m <sup>-3</sup> )
	Measured by thermal infrared imager	Measured by recording thermometer	Calculated by regression equation	Between real value and measured value by infrared imager	Between real value and corrected value			
a	41.2	82.0	76.74	0.496	0.064	85	15	0.99
b	34.3	57.6	49.70	0.406	0.137	150	30	1.15
c	63.8	89.1	84.39	0.284	0.053	100	25	0.58
d	51.4	79.6	71.74	0.354	0.099	125	10	1.74

#### 4 Corresponding relationship between infrared imager and geometry location

The infrared image compared with the surface of the measured object has a certain extent of deformation. The loss of the geometry information limited the appliance of the thermal infrared imager to a certain extent. The visualization grid method was applied to processing the modified results, and the geometric information was obtained. This provided the basis of obtaining measuring points' geometric coordinates.

The grids with the side length of 20 mm were set on the surface of measured object. These grids were visible. The coverage area of these grids was bigger than the scale of measuring points. The coordinate geometry of the nodes of each grid had been measured. The surface of measured object covered by the visible grids was shot by the thermal infrared imager. The temperature information of the knots in the infrared image corresponded to the geometry information. Then the geometry information of the other pixel points which were not located in the knot can be attained by the method of interpolation. The quadratic interpolation method was used to simulate. Figure 7 shows the infrared images measured by the method of visible grids to these four samples of sulfide ores [15–17].

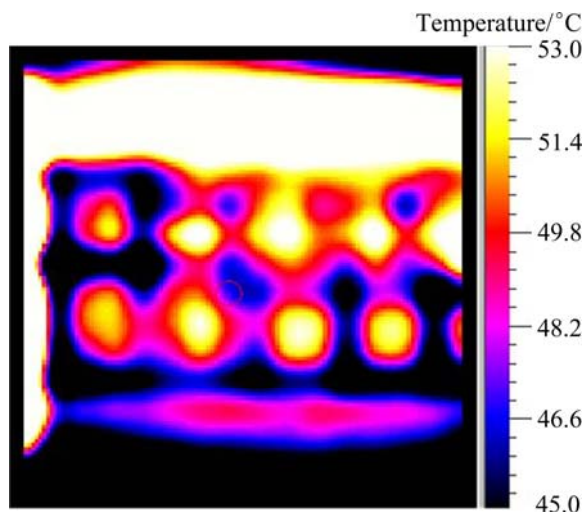


Fig. 7 Visual grid infrared images of sample A

Using the regression equations from Table 7, the temperatures of measuring points 1 to 15 were modified. These values were applied by quadratic interpolation method after modification. The temperature and geometry information of any point on the measured ores surface could be calculated. The geometric coordinates of the measuring points were 1(0,4), 2(2,4), 3(4,4), 4(6,4),

5(8,4), 6(0,2), 7(2,2), 8(4,2), 9(6,2), 10(8,2), 11(0,0), 12(2,0), 13(4,0), 14(6,0) and 15(8,0).

Analyzing the experimental data, after using the quadratic interpolation method, simulating the temperature field of the measured sulfide ores surface, the formulas about the interpolation are obtained as follows.

The interpolation formula of sulfide ore sample A is

$$z=(p_1+p_2x+p_3y+p_4y^2+p_5y^3)/(1+p_6x+p_7x^2+p_8x^3+p_9y+p_{10}y^2) \quad (17)$$

where

$$\begin{aligned} p_1 &= 97.3013642358954, \\ p_2 &= 0.795355574375091, \\ p_3 &= 39.0418893313577, \\ p_4 &= -73.4731450194415, \\ p_5 &= 14.4363774591075, \\ p_6 &= 0.010986245346932, \\ p_7 &= -0.000392818452290724, \\ p_8 &= 3.26529179390053 \times 10^{-5}, \\ p_9 &= -0.794085907441427, \\ p_{10} &= 0.137594689676688. \end{aligned}$$

The degree of fitting of the formula is  $R^2=0.98394$ .

The interpolation formula of sulfide ore sample B is

$$z=(p_1+p_2x+p_3x^3+p_4x^3+p_5y)/(1+p_6x+p_7y+p_8y^2) \quad (18)$$

where

$$\begin{aligned} p_1 &= 96.4759844565897, \\ p_2 &= -1.02191306382297, \\ p_3 &= -0.873112173762358, \\ p_4 &= 0.0499421366919425, \\ p_5 &= -15.1989884563731, \\ p_6 &= -0.0617127535966723, \\ p_7 &= -0.114167794038204, \\ p_8 &= -0.00505186722104378. \end{aligned}$$

The degree of fitting of the formula is  $R^2=0.98394$ .

The interpolation formula of sulfide ore sample C is

$$z=(p_1+p_2x+p_3y)/(1+p_4x+p_5x^2+p_6y+p_7y^2) \quad (19)$$

where

$$\begin{aligned} p_1 &= 90.0819796316795, \\ p_2 &= -8.82615743001834, \\ p_3 &= -38.1162014955155, \\ p_4 &= -0.108623630679033, \\ p_5 &= 0.0011400202711923, \end{aligned}$$

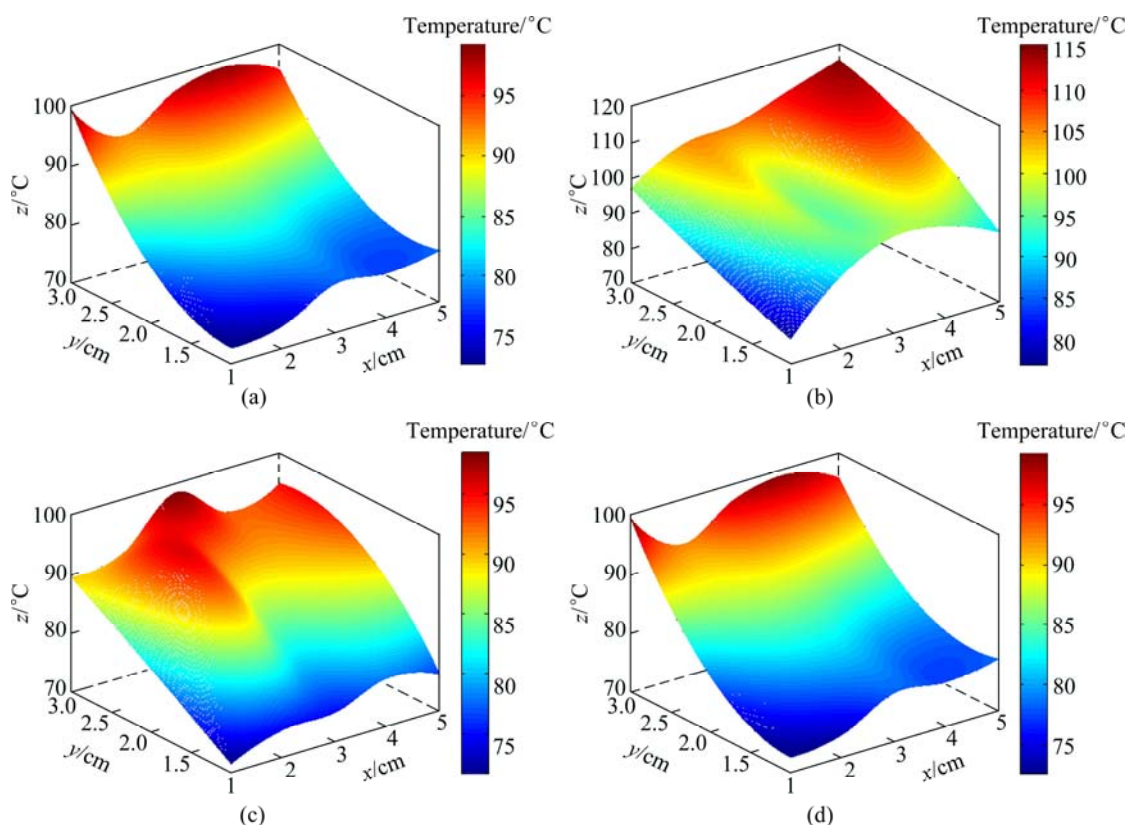


Fig. 8 Temperature curve surface of samples A (a), B (b), C (c) and D (d)

$$p_6 = -0.353551523285118,$$

$$p_7 = -0.0301155082789904.$$

The degree of fitting of the formula is  $R^2 = 0.98394$ .

The interpolation formula of sulfide ore sample D is

$$z = (p_1 + p_2x + p_3x^3 + p_4x^3 + p_5y + p_6y^2) / (1 + p_7x + p_8x^2 + p_9y + p_{10}y^2) \quad (20)$$

where

$$p_1 = 99.2749033238387,$$

$$p_2 = 3444.29416278157,$$

$$p_3 = -5.43916893482505,$$

$$p_4 = -16.6443622100309,$$

$$p_5 = 631324.038655901,$$

$$p_6 = -155240.823252424,$$

$$p_7 = 40.4968651391782,$$

$$p_8 = -2.00653340506251,$$

$$p_9 = 7683.8695978356,$$

$$p_{10} = -1885.20631099843.$$

The degree of fitting of the formula is  $R^2 = 0.98394$ .

$x$  is the abscissa axis of the measured point,  $y$  is the vertical coordinate of the measured point, and  $z$  is the temperature value of the point  $(x, y)$  after using the quadratic interpolation method.

By the method of visible grid, the temperature curve

surface of the sulfide ores was obtained. Figure 8 shows the temperature curve surface of the four sulfide ores.

From the temperature curve surface of the sulfide ores, we can see where is too high in temperature. This provides the basis of actual prediction for the spontaneous combustion of sulfide ores. This method has made up the shortcomings that the temperature information obtained by thermal infrared imager can not correspond to the geometry information precisely or the missing of the geometry information.

## 5 Conclusions

1) The relationship between thermal infrared imager and four factors, including emissivity, distance, angle and dust concentration, was obtained.

2) The regression equations about distance, angle and dust concentration were obtained, which can improve the accuracy of thermal infrared imager.

3) Accurate results were obtained by using the regression equations in practice, but the emissivity of the measured sulfide ores should be measured ahead.

4) The geometry information of the sulfide ores can be corresponded to the temperature information of the infrared image by visible grids. The scope of appliance of thermal infrared imager is extended.

## References

- [1] CARPENTIER O, DEFER D, ANTEZAK E, DUTHOIT B. The use of infrared thermographic and GPS topographic surveys to monitor spontaneous combustion of coal tips [J]. *Applied Thermal Engineering*, 2005, 25: 2677–2688
- [2] MANSOR S B, CRACKNELL A P, SHILIN B V. Monitoring of underground coal fires using thermal infrared data [J]. *International Journal of Remote Sensing*, 1994, 15(8): 1675–1685.
- [3] NINTEMAN D J. Spontaneous oxidation and combustion of sulfide ores in underground mines [R]. *Information Circular 8775*, USA: Bureau of Mines, 1978: 1–40.
- [4] WU C, LI Z J. A simple method for predicting the spontaneous combustion potential of sulfide ores at ambient temperature [J]. *Transaction of the Institutions of Mining and Metallurgy A*, 2005, 114(2): 125–128.
- [5] WU C, XIA C N, LI Z J. Safety assessment system for evaluating spontaneous of sulfide ores in mining stope [C]// *Proceedings of the 2006 International Symposium on Safety Science and Technology*. Changsha, 2006: 1599–1604.
- [6] PAN Wei, WU Chao, LIU Hui, YANG Fu-qiang. Self-heating test of sulfide ore heap and numerical simulation of temperature field [J]. *The Chinese Journal of Nonferrous Metals*, 2010, 20(1): 149–155. (in Chinese)
- [7] LI Luo-ming, WU Chao, YANG Fu-qiang, GAO Ge. Study on relevant factors during measuring sulfide ore pile temperature in the state of self-heating by infrared spectroscopy [J]. *Fire Safety Science*, 2008, 17(1): 49–53. (in Chinese)
- [8] ROSENBLUM F, SPIRA P. Evaluation of hazard from self-heating of sulfide rock [J]. *CIM Bull*, 1995, 88(989): 44–49.
- [9] BOYLE R J, SPUCKLER C M, LUCCI B L, CAMPERCHIOLI W P. Infrared low-temperature turbine vane rough surface heat transfer measurements [J]. *ASME Journal of Turbomachinery*, 2001, 123(1): 168–177.
- [10] SWEENEY P C, RHODES J F. An infrared technique for evaluating turbine airfoil cooling designs [J]. *ASME Journal of Turbomachinery*, 2000, 122(1): 170–177.
- [11] LIU Gao-wen, GUO Yi-ding. Reestablishment of geometric information in surface temperature measurements with infrared thermography [J]. *Infrared Technology*, 2004, 26(1): 56–59. (in Chinese)
- [12] LIU Hui, WU Chao, YANG Fu-qiang, LI Ya-wei. Detection of spontaneous combustion of sulfide ores by infrared thermal imaging method [J]. *Science & Technology Review*, 2010, 28(2): 91–95. (in Chinese)
- [13] SHENG Yao-bin, WANG Yun-jia. Mining spatial information in surface temperature measurements of coal gangue with infrared thermography [J]. *Infrared Technology*, 2007, 29(1): 59–61. (in Chinese)
- [14] YANG Li. Calculation and error analysis of temperature measurement using thermal image [J]. *Infrared Technology*, 1999, 21(4): 20–24. (in Chinese)
- [15] ELMAHDY A H, DEVINE F. Laboratory infrared thermography technique for window surface temperature measurement [J]. *ASHRAE Transactions*, 2005, 111(1): 561–571.
- [16] KAZUYA T, HARUNORI Y, YUZO T. Measurement of thermal environment in Kyoto city and its prediction by CFD simulation [J]. *Energy and Building*, 2004, 36: 771–779.
- [17] TERUMI I, YOSHIZO O. Surface temperature measurement near ambient condition using infrared radiometers with different detection wavelength bands by applying a gray body approximation [J]. *NDT & E International*, 1996, 29(6): 363–369.

# 硫化矿石自燃红外热成像预测技术分析

李孜军, 石东平, 吴超, 王晓磊

中南大学 资源与安全工程学院, 长沙 410083

**摘要:** 针对红外测温法预测硫化矿石自燃的误差大、精度低等问题, 用可记录测温仪和红外热像仪对硫化矿石堆表面温度进行对比测定。分析发射率、距离、角度、粉尘浓度这 4 个影响测温精度的主要因素; 对数据进行处理得到单个影响因素的拟合方程和综合影响因素的拟合方程。同时, 利用可视化网格法和插值法, 解决了传统红外测温中单纯依据红外图像无法用简单公式描述被测表面几何位置的问题, 并建立了红外图像温度和几何位置相对应的关系。

**关键词:** 硫化矿石; 自燃; 预测; 红外测温; 影响因素; 拟合方程; 几何定位

(Edited by YANG Hua)